

In-orbit calibration approach of the MICROSCOPE experiment for the test of the equivalence principle at 10^{-15}

Gregory Pradels and Pierre Touboul

Physics and Instrumentation Department, ONERA, Office National d'Etude et de Recherches Aérospatiales, F-92322 Châtillon Cedex, France

Received 18 February 2003

Published 4 June 2003

Online at stacks.iop.org/CQG/20/2677

Abstract

The MICROSCOPE mission is a space experiment of fundamental physics which aims to test the equality between the gravitational and inertial mass with a 10^{-15} accuracy. Considering these scientific objectives, very weak accelerations have to be controlled and measured in orbit. By modelling the expected acceleration signals applied to the MICROSCOPE instrument in orbit, the developed analytic model of the mission measurement shows the requirements for instrument calibration. Because of on-ground perturbations, the instrument cannot be calibrated in the laboratory and an in-orbit procedure has to be defined. The proposed approach exploits the drag-free system of the satellite and is an important element of the future data analysis of the MICROSCOPE space experiment.

PACS number: 04.80.Cc

(Some figures in this article are in colour only in the electronic version)

1. Introduction

In 1915, Einstein enounced the equivalence principle (EP) as one of the hypotheses of his theory of general relativity, describing the full equivalence between gravity and inertia, and, furthermore, between reference frames under uniform gravity or undergoing accelerations where the same laws of physics are observed. Today, the incompleteness of this theory has been pointed out with respect to quantum physics and has led modern physicists to seek new interactions. Nevertheless these new theories suppose EP violations at levels less than 10^{-12} [1]; a very accurate EP test is then fundamental for their verification. To observe a potential signal of EP violation, tests of the universality of free fall appear to be more promising [2]. Recently, experiments have been performed [3], such as the lunar laser ranging tests [4],

which measure the acceleration ratios between the earth and the moon relative to the sun with a precision of 10^{-12} [5]. Other tests carried out in the laboratory with highly sensitive torsion balance gave accuracies of up to 10^{-13} . However, the very quiet environment offered on board a satellite and the possibility, as demonstrated below, of reducing the gravity gradient effect allows us to achieve an improvement of a few orders of magnitude. This is the goal of the MICROSCOPE space mission which, thanks to the ultra-sensitive accelerometer technology, will target an EP test accuracy of 10^{-15} .

2. The MICROSCOPE space mission

2.1. Mission overview

The MICROSCOPE (MICROSatellite pour l'Observation du Principe d'Equivalence) space mission has been selected by CNES, in cooperation with ESA, and is the first project to perform an EP test in orbit. The satellite will be launched in 2006 and is equipped with the new technology of the field emission electric propulsion (or FEEP) thrusters now available in Europe and necessary for the permanent control of the satellite attitude and orbit. Its weight will not exceed 150 kg for a payload power of less than 40 W. The mission is planned to have a one year duration. The EP test will be performed with a dedicated differential accelerometer developed by ONERA in France, whose technology has been assessed in space in previous missions [6–8]. The satellite will be injected onto a sun-synchronous and quasi-polar orbit with an altitude of about 700 km. The experiment on board the MICROSCOPE satellite is similar to a Galileo test with two test masses made of different materials in quasi-unlimited free fall around the earth [9].

2.2. The MICROSCOPE payload

The payload of the satellite is composed of two differential accelerometers each including two electrostatic inertial sensors operating independently. Both differential accelerometers are identical except that one contains test masses of different materials while both masses of the other one are of the same material. The comparison between the measurements of these two instruments will help us to reject systematic errors.

The operation of each inertial sensor is as follows: the six degrees of freedom of the inertial mass are permanently controlled by combinations of electrostatic pressures applied to it with a set of electrodes. The EP test will be performed along the axis of revolution of the configuration (X -axis). Motions of the test masses are measured along with a resolution of $6 \times 10^{-10} \text{ m Hz}^{-1/2}$ and controlled with a resolution better than $2.5 \times 10^{-12} \text{ m/s}^2/\sqrt{\text{Hz}}$ [10]. Taking into account the value of the instrument's maximum measurement range ($5 \times 10^{-7} \text{ m s}^{-2}$ in high-resolution mode), a drag-free and attitude control system (DFACS) combines the outputs of the accelerometers and the star sensor to reduce the non-gravitational forces applied to the satellite. This system estimates the thrust to be continuously applied by the thrusters in order to limit the level of the instrument linear acceleration to $3 \times 10^{-10} \text{ m/s}^2/\sqrt{\text{Hz}}$ and the angular acceleration to $10^{-8} \text{ rad/s}^2/\sqrt{\text{Hz}}$ at the frequency of the space experiment. FEEP thrusters have been selected: these are advanced electrostatic thrusters able to deliver thrust at a μN level with high accuracy [11].

For the selection of the material of the two test masses, a compromise between the theoretical interests (nuclei property) and the material property has been made by selecting a platinum–titanium couple [12].

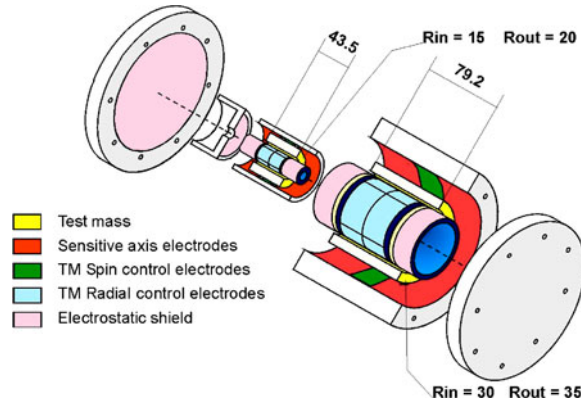


Figure 1. Schema of a differential accelerometer composed of two cylindrical inertial sensors, themselves composed of three cylinders: a test mass (in yellow) surrounded by two cylinders of electrodes.

(This figure is in colour only in the electronic version)

2.3. In-orbit measurement

In a free-fall experiment, a violation of the equivalence principle leads to the observation of the non-equality between the ratios of the gravitational and the inertial mass (m_g and m_i) for two bodies made of different materials and submitted to the same gravity field. Let us note δ , the EP violation parameter: $\delta = (m_g/m_i)_{\text{mass 1}} - (m_g/m_i)_{\text{mass 2}}$. Considering the inertial sensor in O_1 , the acceleration output is simply expressed by

$$\vec{\Gamma}_{\text{meas}} = \frac{\vec{F}_e}{m_i} \approx \frac{\partial^2 \vec{x}_1}{\partial t^2} - \frac{m_g}{m_i} \cdot \vec{g}(O_1), \quad (1)$$

where F_e is the electrostatic force applied to the test mass by the electrodes, g is the earth's gravitational field and x_1 is the test-mass position with respect to the inertial reference frame.

For a differential accelerometer, the equation of the measurement is computed using the difference between each inertial sensor outputs

$$\vec{\Gamma}_{\text{measured,diff}} \approx \delta \cdot \vec{g}(o) + [T] \cdot \overrightarrow{O_1 O_2}, \quad (2)$$

where $[T]$ is the earth's gravity gradient, and O is the centre of $O_1 O_2$ considering the two test masses controlled in the same motion. Although the major line of the earth gradient signal is situated at twice the orbital frequency, at the EP frequency there exists a smaller line whose amplitude is proportional to the eccentricity [13] or induced by the non-ellipsoid geoid. To reach an accuracy of 10^{-15} , the second term of the last equation must then be reduced either by limiting the distance between the two masses or the amplitude of the orbital eccentricity.

The average of both inertial sensor outputs provides an estimation of the mean acceleration undergone by the satellite and counteracted by the DFACS.

Previous experiments in space, such as the CHAMP mission, offered the possibility of studying some of the accelerometric perturbations occurring on a small satellite at low altitude (500 km in the case of CHAMP). In the MICROSCOPE mission, particular care has been taken to limit these disturbances. For instance, a sun-synchronous orbit with no shadow crossing period has been selected, the satellite is compact and stiff, and the inner thermal control is passive. The developed techniques [14] to suppress the disturbance peak signals and to detect and analyse the non-stationary ones are useful for MICROSCOPE data processing: the EP

signal is a stationary, quite sine wave shape according to the rotation of the $\vec{g}(o)$ field in the instrument frame.

3. Calibration approach for the MICROSCOPE accelerometer

In relation to the perturbation studies of previous missions, the scientific measurements made on the MICROSCOPE mission might be disturbed through the intrinsic defects of the instrument. An analysis is here performed to characterize the instrument's calibration.

The principle of operation of the differential accelerometer needs centred test masses between pairs of electrodes but neither the test masses nor the electrodes are perfectly cylindrical, positioned and aligned: a $2 \mu\text{m}$ tolerance has been specified for the geometry of each part. These defects might introduce harmonics or random signals higher than the required limit of a few $10^{-15} \text{ m s}^{-2}$, although the amplitudes of the disturbing forces (non-gravitational forces, earth's gravity gradient) are reduced by the DFACS or by an in-orbit recentering of the test masses. A calibration procedure for the instrument is then necessary to measure the amplitudes of these defects and correct the scientific measurements by an *a posteriori* data treatment.

3.1. Linear model of the instrument

Let us consider the following linear model of one inertial sensor i (with three degrees of freedom):

$$\Gamma_{\text{measured},i} = K_{0,i} + M_i \Gamma_{\text{excitation},i} + \Gamma_{\text{noise},i} \quad \text{with} \quad M_i = K_{1i} O_i S_i \quad (3)$$

where $K_{0,i}$ is the intrinsic bias of the instrument due to cage dissymmetries and potential offsets, M_i is the instrument sensitivity matrix and $\Gamma_{n,i}$ is the instrument intrinsic noise. The sensitivity matrix M_i is deduced from the product of a coupling matrix (S_i), an orthogonal matrix (O_i) and a diagonal matrix ($K_{1,i}$). $K_{1,i}$ represents the scale factors of the instrument along the three axes. O_i is a matrix of rotation between the inertial sensor frame and the satellite star sensor reference frame. S_i matrix represents the coupling elements between the instrument axis, induced in particular by the perpendicularity defects of the test mass (figure 2). Considering the amplitudes of the matrix elements (1 ± 10^{-2} for the scale factors, 10^{-2} rd for the misalignments and 10^{-3} for the couplings), this equation can be approximated by

$$\Gamma_{\text{measured},i} = K_{0,i} + (I + dK_{1,i} + dO_i + dS_i) \Gamma_{\text{excitation},i} + \Gamma_{\text{noise},i}. \quad (4)$$

From (4), the differential accelerometer measurement is expressed by introducing what are called the differential mode, $\Gamma_{\text{meas,diff}}$, (half the difference between the two sensor outputs) and the common mode, $\Gamma_{\text{meas,com}}$, (half the sum) and by considering M_{com} and M_{diff} the matrices representing, respectively, the common and the differential mode of the instrument sensitivity matrices:

$$\begin{pmatrix} \Gamma_{\text{meas,com}} \\ \Gamma_{\text{meas,diff}} \end{pmatrix} = \begin{pmatrix} K_{0,\text{com}} \\ K_{0,\text{diff}} \end{pmatrix} + M \begin{pmatrix} \Gamma_{\text{app,com}} \\ \Gamma_{\text{app,diff}} \end{pmatrix} + \begin{pmatrix} \Gamma_{\text{noise,com}} \\ \Gamma_{\text{noise,diff}} \end{pmatrix} \quad \text{with} \quad (5)$$

$$M = \begin{pmatrix} I + dM_{\text{com}} & M_{\text{diff}} \\ M_{\text{diff}} & I + dM_{\text{com}} \end{pmatrix}$$

$$dM_{\text{com}} = I + dK_{1,\text{com}} + dO_{\text{com}} + dS_{\text{com}} \quad M_{\text{diff}} = K_{1,\text{diff}} + dO_{\text{diff}} + dS_{\text{diff}}$$

$$dK_{1,\text{com}} = \frac{dK_{1,1} + dK_{1,2}}{2} \quad dK_{1,\text{diff}} = \frac{dK_{1,1} - dK_{1,2}}{2} \quad \text{and so on for } dO \text{ and } dS.$$

Note that the differential mode is computed for commodity in (5) by half the difference of the accelerations in contrast to (2) which is the full difference. The first line of (5) expresses the

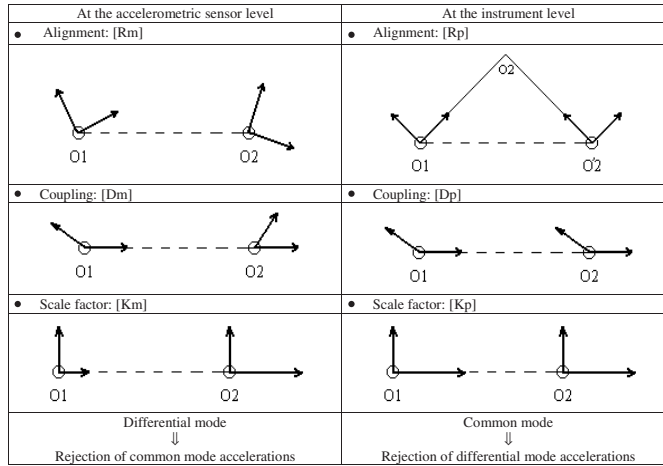


Figure 2. The intrinsic defects of the differential accelerometer are decomposed in three categories and two modes. The misalignments are typically due to the positioning and the orientations between the concentric cylinders composing the instrument, the couplings due to their geometrical defects and the scale factor errors due to the defects of the electrode areas.

measurement used for the drag-free control, and the second the measurement for the EP test. In the latter, the instrument differential-mode defects introduce the satellite common-mode acceleration (residual drag) while the instrument common-mode defects introduce the satellite differential-mode acceleration (gravity gradient, attitude motions depending on the distance between the two masses).

For a signal-to-noise ratio of one and the 10^{-15} EP test accuracy, the differential acceleration measurement must be $8 \times 10^{-15} \text{ m s}^{-2}$ for the 700 km altitude. The total error level occurring at the same frequency and phase as the signal to be detected must thus be lower than $8 \times 10^{-15} \text{ m s}^{-2}$.

Different sources of disturbances have been identified in addition to the couplings and misalignments such as the satellite self-gravity, the radiometer effect and the thermal pressure. A total level of $10^{-15} \text{ m s}^{-2}$ has been specified for all signals introduced by dM_{com} and M_{diff} matrices and the same amplitude for the disturbance signal due to the earth's gravity gradient and the residual distance between both test masses. Consequently, the calibration goal consists in measuring the amplitude of this distance, dM_{com} and M_{diff} matrices in order to correct by a later treatment the differential measurement along the EP test axis.

From (5), the in-orbit calibration of the instrument consists in estimating the matrix M^{-1} in order to correct the measurement acceleration, Γ_{meas} , and so obtain the true acceleration, Γ_{real} . It is thus more efficient to evaluate directly the useful components of the inverse matrix M^{-1} , noted A , than to evaluate and inverse M . The matrix A can be expressed by

$$\begin{pmatrix} \Gamma_{\text{app},c} \\ \Gamma_{\text{app},d} \end{pmatrix} = \begin{pmatrix} A_c & A_d \\ A_d & A_c \end{pmatrix} \left[\begin{pmatrix} \Gamma_{\text{meas},c} \\ \Gamma_{\text{meas},d} \end{pmatrix} - \begin{pmatrix} \Gamma_{\text{noise},c} \\ \Gamma_{\text{noise},d} \end{pmatrix} - \begin{pmatrix} K_{0,c} \\ K_{0,d} \end{pmatrix} \right]. \quad (6)$$

This equation can be considered as the fundamental equation of the calibration procedure.

3.2. Required performance for the instrument calibration

To establish the calibration objectives, a typical MICROSCOPE orbit has been computed in detail [15] with 10^{-2} mean eccentricity, 98.4° inclination and 720 km altitude leading to

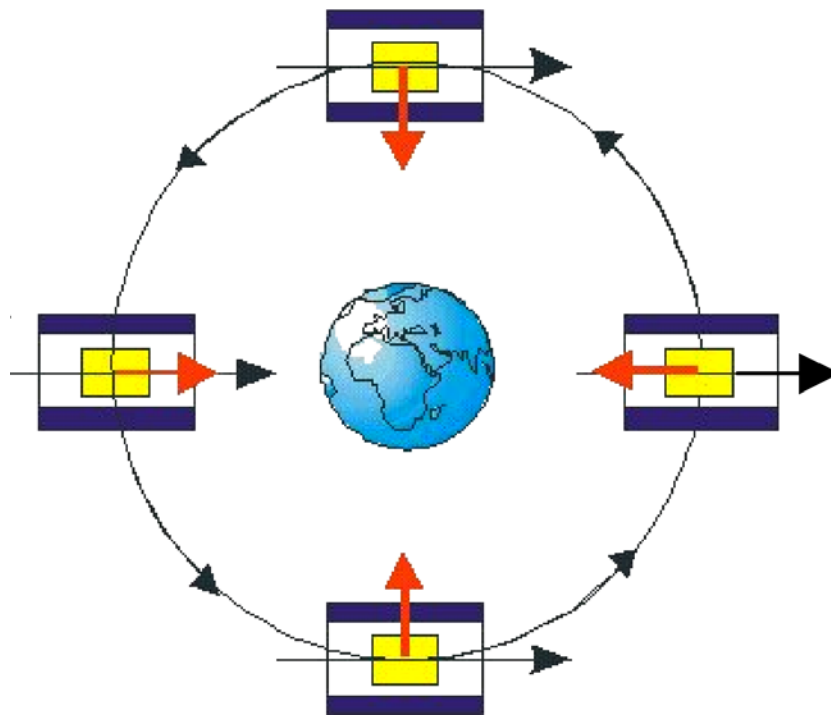


Figure 3. Two concentric masses orbit around the earth. Subjected to the same gravitational field of the earth an eventual signal of EP violation is measured through the necessary (or unnecessary in the case of no violation) electrostatic forces to be added in such a way that the two masses have the same orbit.

Table 1. Earth's gravitational field and gravity gradient expressed in the measurement frame for a typical MICROSCOPE orbit. These values have been computed with the support of the Observatoire de la Côte d'Azur's models. Y is normal to the orbital plane, and X and Z are in this plane.

Earth's gravity field	X	Y	Z			
dc (m s^{-2})	5.8×10^{-6}	3.4×10^{-4}	5.1×10^{-6}			
Orbital frequency (m s^{-2})	7.9	2.6×10^{-3}	7.9			
Gravity gradient	XX	XY	XZ	YY	YZ	ZZ
dc ($/\text{s}^2$)	5.6×10^{-7}	3.4×10^{-8}	1.4×10^{-10}	1.1×10^{-6}	5.3×10^{-8}	5.6×10^{-7}
Orbital frequency ($/\text{s}^2$)	9.3×10^{-9}	3.2×10^{-11}	9.5×10^{-9}	3.4×10^{-8}	3.6×10^{-11}	2.5×10^{-8}

a near 8 m s^{-2} gravitational acceleration signal. Table 1 presents the absolute amplitude of the gravitational and non-gravitational accelerations expressed along the inertial axis of the instrument and at the orbital frequency F_O ($8 \times 10^{-4} \text{ Hz}$). These data are hereafter used to perform the harmonic analysis of the measured signal. Note that the self-gravity of the satellite is neglected and that many other lines appear as observed hereafter in the simulations when considering all spherical harmonics of the earth's gravity potential. The EP test signal is along the earth field, and thus projected onto the instrument inertial axes at the orbital frequency (figure 3). Table 2 shows the specified performance of the DFACS [17]. From these tables and from (2), the acceleration amplitudes, measured by a perfect differential accelerometer, are

Table 2. Requirements for the performance of the drag-free system (DFACS) used to reduce the amplitude of non-gravitational accelerations suffered by the satellite.

	X	Y	Z
Angular velocity			
dc (rd s ⁻¹)	10 ⁻⁵	1.07 × 10 ⁻³	10 ⁻⁵
Fluctuations (rd/s/√Hz)	10 ⁻⁶	10 ⁻⁶	10 ⁻⁶
Angular acceleration			
dc (rd s ⁻²)	2 × 10 ⁻⁶	2 × 10 ⁻⁶	2 × 10 ⁻⁶
Fluctuations (rd/s ² /√Hz)	10 ⁻⁸	10 ⁻⁸	10 ⁻⁸
Linear acceleration			
dc (m s ⁻²)*	10 ⁻⁹	10 ⁻⁹	10 ⁻⁹
Fluctuations (m/s ² /√Hz)	3 × 10 ⁻¹⁰	3 × 10 ⁻¹⁰	3 × 10 ⁻¹⁰

* When the DFACS is not disturbed by the accelerometer bias level.

Table 3. The signals measured by a perfect differential accelerometer are computed for common and differential modes considering two values of the distance between the two test masses along the X and Z axes.

	Mean applied signal		Applied signal difference		
	X	YZ	X	Y	Z
$\Delta x, y, z = 20 \mu\text{m}$					
dc (m s ⁻²)	10 ⁻⁹	10 ⁻⁹	-1.1 × 10 ⁻¹¹	-2.1 × 10 ⁻¹¹	-1.16 × 10 ⁻¹¹
Orbital frequency (m s ⁻²)	10 ⁻¹²	10 ⁻¹²	1.8 × 10 ⁻¹³	6.9 × 10 ⁻¹³	5.0 × 10 ⁻¹³
Fluctuations (m/s ² /√Hz)	3 × 10 ⁻¹⁰	3 × 10 ⁻¹⁰	4 × 10 ⁻¹³	3 × 10 ⁻¹³	5 × 10 ⁻¹³
$\Delta x, z = 0.1 \mu\text{m}$					
$\Delta y = 20 \mu\text{m}$					
dc (m s ⁻²)	10 ⁻⁹	10 ⁻⁹	-4.0 × 10 ⁻¹¹	-2.2 × 10 ⁻¹¹	4.0 × 10 ⁻¹¹
Orbital frequency (m s ⁻²)	10 ⁻¹²	10 ⁻¹²	1.5 × 10 ⁻¹⁵	6.9 × 10 ⁻¹³	2 × 10 ⁻¹⁵
Fluctuations (m/s ² /√Hz)	3 × 10 ⁻¹⁰	3 × 10 ⁻¹⁰	2 × 10 ⁻¹³	2 × 10 ⁻¹⁴	2 × 10 ⁻¹³

computed for two values of the distance between the two test masses at dc value, harmonics at F_O and fluctuations (table 3).

With 10⁻² orbit eccentricity, the earth's gravity tensor presents components with high amplitude at orbital frequency, up to a few 10⁻⁸ m/s²/m. Multiplied by the 20 μm distance between the two test masses, this leads to a differential signal of a few 10⁻¹³ m s⁻² (table 3) is reduced to less than 10⁻¹⁵ m s⁻² by the estimation of the common misalignments and couplings.

Table 4 presents the amplitude instrument parameters obtained from the manufacturing and integration specifications. Absolute sensitivity of the instrument cannot be tested in the laboratory because of the range of operation, and the evaluation accuracy is limited by the mass to electrodes accuracy. Alignments and coupling values must be considered with respect to part sizes of a few centimetres, leading then to micrometre machining accuracy when considering the addition of geometry error sources and margins [16]. The amplitude of the signal due to dM_{com} and M_{diff} in the difference of the measured accelerations is provided at the EP test frequency in table 5. With a realistic 20 μm distance between the two test masses after the instrument switches on, the gravity gradient signal (major term of the applied

Table 4. Expected values of the instrument defects deduced from machining and integration tolerances.

Matrix elements	Expected values
I + dK_c	1 ± 10^{-2}
dO_c (rd) dS_c	$\pm 10^{-2}$ $\pm 10^{-4}$
dK_d	$\pm 10^{-2}$
dO_d (rd) dS_d	$\pm 10^{-3}$ $\pm 10^{-4}$

Table 5. The instrument measurement along the EP test axis is computed taking into account the matrices of sensitivity before calibration. From these values the minimum accuracy required for the evaluation of the dM_{com} and M_{diff} matrix is deduced.

Matrix elements	$\Delta x, z = 0.1 \mu\text{m}$	
	$\Delta x, y, z = 20 \mu\text{m}$	$\Delta y = 20 \mu\text{m}$
dK_c	1.86×10^{-15}	0.93×10^{-17}
$(dO_c + dS_c)$	11.8×10^{-15}	6.83×10^{-15}
dK_d	10×10^{-15}	10×10^{-15}
$(dO_d + dS_d)$	2.0×10^{-15}	2.0×10^{-15}
Sum	25.7×10^{-15}	18.8×10^{-15}
Applied difference	1.86×10^{-13}	0.95×10^{-15}
Measured difference	2.12×10^{-13}	0.20×10^{-13}

acceleration) is much too important. Table 5 shows also that a centring with an accuracy of $0.1 \mu\text{m}$ is compatible with the EP test accuracy of 10^{-15} . This centring can only be performed through the ground data processing, i.e. subtracting the gravity gradient signal after evaluation of the off-centring. From table 5, the 3.5×10^{-4} selected specification of accuracy for the evaluation of the dM_{com} matrix (dK_c, dO_c) is deduced when a $20 \mu\text{m}$ distance (by construction) is considered limiting the disturbance terms to $5 \times 10^{-16} \text{ m s}^{-2}$. The elements of the M_{diff} matrix (dK_d, dO_d) must be evaluated with a 1.5×10^{-4} accuracy to limit the perturbing terms at the same level.

In the MICROSCOPE experiment, the estimation of the common scale factor dK_c does not appear necessary for the rejection of the disturbances, which is coherent with the detection of a weak signal (the EP signal) without the absolute scale factor of the measure: the violation signal can be detected but with the relative accuracy of 1% that corresponds to dK_c and that is sufficient.

The importance of the calibration of the common-mode matrix dO_c comes from the high level of the gravity tensor at the frequency of the test due to the 10^{-2} eccentricity. The required calibration performances of this matrix depend thus on the distance amplitude between the two test masses as indicated previously. In case the satellite is rotating about the normal to the orbit, the major lines of the gravity tensor are modulated and separated from the frequency of the EP signal which becomes equal to the sum (or difference) of the orbital frequency and the satellite spin frequency. Then by performing the same analysis, it is easy to show that only dK_d and dO_d have to be calibrated with a 3×10^{-4} accuracy.

3.3. In-orbit calibration procedure

On-ground differential misalignment, couplings and scale factor matching cannot be calibrated even with the anti-seismic test bench developed in the laboratory because of the residual level

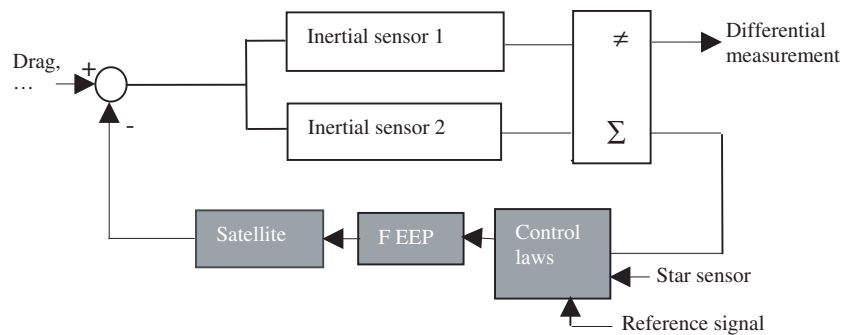


Figure 4. Schema of the DFACS loop using one or both inertial sensor outputs. For the calibration method, reference signals are introduced in the control laws to be followed by the measured values; the sensor sensitivities are then deduced from the comparison of the outputs not directly affected by the reference signal.

of perturbations (few $10^{-9} \text{ m/s}^2/\sqrt{\text{Hz}}$) and the presence of normal gravity. Free-fall tests can also be performed at the Drop Tower in Bremen (Germany) with fall durations of 4.7 s. But the level of the present measured random signal (a few $10^{-7} \text{ m/s}^2/\sqrt{\text{Hz}}$) is too important for high calibration sensitivity [18]. In addition, common misalignment between accelerometers and the star sensor can only be measured after integration in the satellite. An in-orbit calibration procedure must be thus developed.

The first difficulty for in-orbit calibration comes from the lack of well-known signals. The proposed solution for the MICROSCOPE mission consists in applying successive accelerations thanks to the drag compensation system. By the introduction of a reference periodic signal in the DFACS control loop of the orbit motion, the satellite and the instrument are shaken in translation (common mode). By the introduction of the signal in the attitude control loop, the instrument is shaken in rotation (differential mode). This operation is very interesting for the calibration because the misalignments between the accelerometer and the thrusters are rejected by the DFACS loop gains (see figure 4). Another solution consists in using the earth's gravity gradient as a well-known (through a spherical harmonics model) differential signal to calibrate dM_{com} and the distance between the test masses. The advantage of this method is the possibility that it can be exploited all the time; however, the full sensitivity matrix cannot be calibrated. With the DFACS, three common-mode and three differential-mode excitations are generated by applying three periodic translations and three rotations. At frequencies of a few 10^{-3} Hz , from equation (6) five relations can then be deduced for the determination of the X differential line (corresponding to the EP test line) of the matrix A , by considering that the acceleration $\Gamma_{\text{real,diff}}$ is quite null along X . These relations provide in particular the three differential sensitivities (A_{diff}). A last equation is obtained through another line of the measurement vector to deduce the three common misalignments (dO_c).

This method prohibits the determination of the instrument absolute scale factor dKc . The relative accuracies of the estimates of the other matrices are directly defined by dKc . The *a priori* knowledge of the scale factors is 10^{-2} and thus sufficient to evaluate the misalignments from 10^{-2} rd or 10^{-3} rd to $3.5 \cdot 10^{-4} \text{ rd}$ or $1.5 \cdot 10^{-4} \text{ rd}$ required accuracy. As already discussed above, the impossibility of estimating the absolute scale factor is not a limitation for the success of the mission.

The DFACS sensor loop can operate from a linear combination of the outputs of both inertial sensors or from only one of the two sensors. Both configurations are quite similar in their implementation on the propulsion system and in the inertial sensor data process but

Table 6. Comparison between the inverse of the input values of the instrument defects and their estimation for the X -axis. The required accuracy of 3×10^{-4} is obtained.

	Initial value	Estimated value	Absolute difference
$dA_d(1, 1)$	-22.3×10^{-4}	-21.9×10^{-4}	-0.43×10^{-4}
$dA_d(1, 2)$	-1.54×10^{-4}	-1.19×10^{-4}	-0.34×10^{-4}
$dA_d(1, 3)$	2.33×10^{-4}	2.87×10^{-4}	0.53×10^{-4}

the drag-free point can be settled from the centre of one mass to the other one. The attitude motion of the satellite does not offset the sensors in the same way.

Let us define now the necessary amplitudes and frequencies of the necessary calibration signals. For the determination of the A_d coefficients, the amplitude and the frequency of the common excitation signals are selected considering the operating range and bandwidth of the sensors. A frequency of 5×10^{-3} Hz is a good compromise between the EP signal frequency (one or a few orbital frequencies) and the systematical error frequency due to the earth's gravity gradient major lines in such a way that the total systematical error equals the absolute scale factor error, i.e. 10^{-4} (table 4). The duration of the integration necessary to reach the required calibration accuracy is estimated by considering the measurement resolution and the satellite drag-free performance, leading to a total of random signal of $3.8 \times 10^{-12} \text{ m/s}^2/\sqrt{\text{Hz}}$ at 5×10^{-3} Hz. With an excitation amplitude of 10^{-8} m s^{-2} and an integration period of the measured signal extended to 600 s, the A_d matrix coefficient can be evaluated with the required 1.5×10^{-4} accuracy. Simulations of the satellite and instrument operations have been performed with Matlab software to configure these values. Spectral analysis at the calibration frequency has been implemented for the calibration signal extraction.

The common coefficient A_c are much more difficult to evaluate because of the weak amplitude of the generated differential signal or the natural gravity gradient signal with the maximum $20 \mu\text{m}$ off-centring (a few $10^{-11} \text{ m s}^{-2}$). The pointing of the satellite is controlled from the star sensor output and velocity vector from the hybridization estimator exploiting the star sensor and inertial sensor outputs. The ac matrix coefficients concern in particular the attitude of the sensor axes to be determined with respect to the star sensor frame. Thus, the calibration frequency must be sufficiently low where the satellite attitude follows the star sensor outputs. With a frequency of 4×10^{-3} Hz and a maximum angular motion of $\pm 10^\circ$ the expected accuracy can be achieved after an integration period of 50 000 s, i.e. ten orbits.

3.4. Calibration tests with a dedicated simulator

A specific simulator of the DFACS loop with six degrees of freedom has been developed with the software MatLab/Simulink to test the proposed calibration method for different types of orbit and environmental conditions. The simulator includes the sensor matrices of sensitivity and their detailed resolution versus frequency, the overall transfer function of the DFACS, the thruster misalignments and gains. The accelerations suffered by the satellite at the input of the drag-free loop have been computed independently along the orbit [19].

The sensitive matrices of each inertial sensor are randomly drawn in accordance with table 4. Figure 5 presents the Fourier transform (modulus) of the differential-mode measurement performed along the EP test axis (X) with a time window of 4096 s and when the 10^{-8} m s^{-2} common-mode excitation along X is produced. From this measurement the first element of the matrix A_d can be estimated.

All cases of excitations have been simulated and table 6 provides the obtained calibration accuracy for matrix A_d with an integration time of 4096 s, a 10^{-2} eccentricity of the inertial

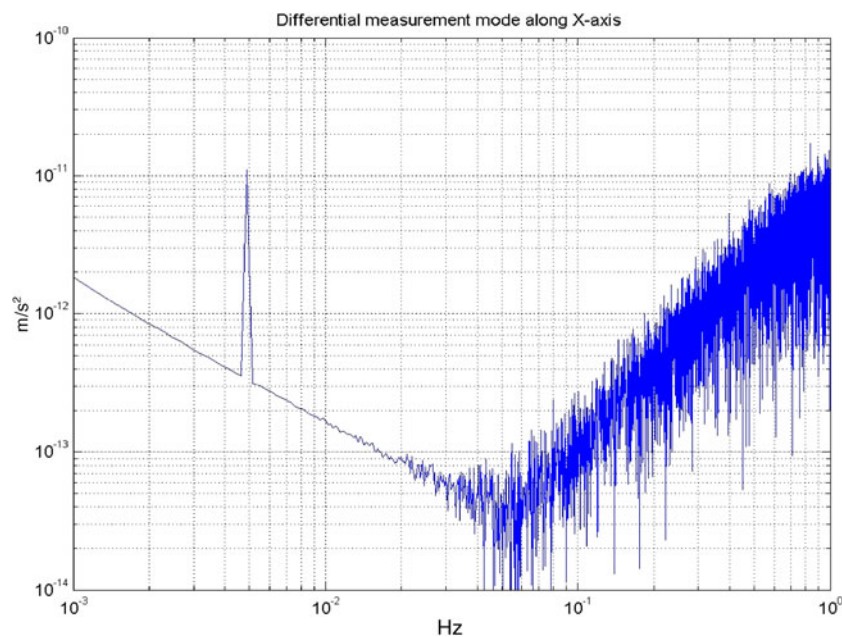


Figure 5. Fourier transform of the differential measurement of the ultra-sensitive X -axis computed by the simulator. These data have been obtained after 4096 s of integration with a sampling frequency of 8 Hz. At low frequency, we observe the earth's gravity gradient components and at 5×10^{-3} Hz the peak due to the linear excitation introduced by the difference of the inertial sensor sensitivity. At upper frequencies the residual non-gravitational accelerations out of the DFACS bandwidth are observed.

orbit and $20 \mu\text{m}$ distance between the two test masses being considered. The results confirm the possibility of calibrating the instrument in orbit with the required precision of 1.5×10^{-4} . The same type of results is obtained with dA_c coefficients.

4. Conclusion

The MICROSCOPE space mission aims to carry out the EP test with an accuracy better than 10^{-15} . In spite of the previous space missions exploiting electrostatic accelerometers developed from the same concept by the laboratory, this mission is an actual technological challenge with very high sensitivity instrumentation, including a specific cylindrical configuration, accommodated on board a drag-free satellite.

The MICROSCOPE drag-free system and the differential measurement between two accelerometers allow us to reach very weak levels of acceleration, compatible with the mission performances. Nevertheless, the instrument outputs need to be finely calibrated in such a way as to interpret the observed signal and to confirm the experiment results. Taking into account the environment of the instrument, the procedures for calibrating both inertial sensors have been proposed and an accuracy of better than 1.5×10^{-4} has been demonstrated by simulation. The interest of the approach is to take advantage of the existing drag-free propulsion system leading to a sufficient performance in a reasonable data observation time.

The developed simulator prepares also the analysis of the data that will be collected after the satellite launch foreseen in 2006. The proposed approach is also convenient for other space missions based on comparison of inertial sensor outputs, e.g. LISA, the space

gravitational wave detector of ESA or STEP, a more ambitious EP test experiment in space. For earth observation missions such as the US GRACE geodesic satellites or the ESA GOCE gradiometric project, weak acceleration and attitude motions of the satellite have also to be finely controlled.

Acknowledgments

The authors would like to express their gratitude to Gilles Metris, who computes the data necessary for this work, for exciting scientific exchanges, and also the MICROSCOPE team members at ONERA.

References

- [1] Damour T 2002 Runaway dilaton and equivalence violations IHES/P/02/27, Bicocca FT-02-7, CERN-TH/2002-092
- [2] Damour T 2001 Questioning the equivalence principle *C. R. Acad. Sci., Paris IV* **2** 1249
- [3] Dittus H and Mehls C 2001 A new experiment baseline for testing the weak equivalence principle at the Bremen drop tower *Class. Quantum Grav.* **18** 2417–25
- [4] Williams J G, Newhall X X and Dickey J O 1996 *Phys. Rev. D* **53** 6730
- [5] Baessler S *et al* 1999 Improved test of the equivalence principle for the gravitational self-energy *Phys. Rev. Lett.* **13** 3585
- [6] Touboul P *et al* ASTRE accelerometer. Verification tests in drop tower Bremen ONERA, 1994-124
- [7] Reigber Ch 2002 CHAMP mission status *Adv. Space Res.* **30** 129–34
- [8] Touboul P *et al* 1996 Electrostatic space accelerometer for present and future missions *Class. Quantum Grav.* **13** A67
- [9] Touboul P and Rodrigues M 2001 MICROSCOPE, testing the equivalence principle in space *C. R. Acad. Sci., Paris IV* **2** 1271–86
- [10] Chuun R *et al* 2002 MICROSCOPE mission and performance *Nucl. Phys. B* **113** 277–81
- [11] Marcuccio S and Giannelli S 1997 Attitude and orbit control of small satellites and constellations with FEED thrusters IEPC-97-188 *Proc. 25th Electric Propulsion Conf. (Cleveland, OH, 1997)*
- [12] Blaser J P 1996 Tests-mass material selection for STEP *Class. Quantum Grav.* **13** A87
- [13] Metris G 2002 Expression du vecteur acceleration de gravité et du tenseur gradient de gravité en repère instrument *Technical Note* October 2002
- [14] Pradels G 2003 Feedbacks from CHAMP mission at press
- [15] Metris G 2002 Simulations et analyses pour la mission MICROSCOPE Private communication
- [16] Aversa N *et al* Complément d'étude SCAO de la phase A MICROSCOPE, ASTRIUM EAA.NT.XS.3684432.02
- [17] Lafargue L 2002 Configuration mécanique d'accéléromètres électrostatiques pour le test en orbite du Principe d'Equivalence *PhD Thesis*
- [18] Rodrigues M 2002 MICROSCOPE, test of the universality of mass free fall in a well controlled in-orbit environment IAF
- [19] Pradels G and Touboul P Specifications for the calibration of the MICROSCOPE differential accelerometer RT 1/06806 DMPH